Atmospheric volatile organic compound measurements during the Pittsburgh Air Quality Study: Results, interpretation, and quantification of primary and secondary contributions

Dylan B. Millet,[1,2] Neil M. Donahue,[3] Spyros N. Pandis,[3] Andrea Polidori,[4] Charles O. Stanier,[2,5] Barbara J. Turpin,[4] and Allen H. Goldstein[1]

Received 3 February 2004; revised 7 April 2004; accepted 22 April 2004; published 25 January 2005.

[1] Primary and secondary contributions to ambient levels of volatile organic compounds (VOCs) and aerosol organic carbon (OC) are determined using measurements at the Pittsburgh Air Quality Study (PAQS) during January–February and July–August 2002. Primary emission ratios for gas and aerosol species are defined by correlation with species of known origin, and contributions from primary and secondary/biogenic sources and from the regional background are then determined. Primary anthropogenic contributions to ambient levels of acetone, methylethylketone, and acetaldehyde were found to be 12–23% in winter and 2–10% in summer. Secondary production plus biogenic emissions accounted for 12–27% of the total mixing ratios for these compounds in winter and 26–34% in summer, with background concentrations accounting for the remainder. Using the same method, we determined that on average 16% of aerosol OC was secondary in origin during winter versus 37% during summer. Factor analysis of the VOC and aerosol data is used to define the dominant source types in the region for both seasons. Local automotive emissions were the strongest contributor to changes in atmospheric VOC concentrations; however, they did not significantly impact the aerosol species included in the factor analysis. We conclude that longer-range transport and industrial emissions were more important sources of aerosol during the study period. The VOC data are also used to characterize the photochemical state of the atmosphere in the region. The total measured OH loss rate was dominated by nonmethane hydrocarbons and CO (76% of the total) in winter and by isoprene, its oxidation products, and oxygenated VOCs (79% of the total) in summer, when production of secondary organic aerosol was highest.

Citation: Millet, D. B., N. M. Donahue, S. N. Pandis, A. Polidori, C. O. Stanier, B. J. Turpin, and A. H. Goldstein (2005), Atmospheric volatile organic compound measurements during the Pittsburgh Air Quality Study: Results, interpretation, and quantification of primary and secondary contributions, *J. Geophys. Res.*, *110*, D07S07, doi:10.1029/2004JD004601.

1. Introduction

[2] Airborne particulate matter (PM) can adversely affect human and ecosystem health, and exerts considerable influence on climate. Effective PM control strategies require an understanding of the processes controlling PM concentration and composition in different environments. The Pittsburgh Air Quality Study (PAQS) is a comprehensive, multidisciplinary project directed at understanding the processes governing aerosol concentrations in the Pittsburgh region [e.g., *Wittig et al.*, 2004a; *Stanier et al.*, 2004a, 2004b]. Specific objectives include characterizing the physical and chemical properties of regional PM, its morphology and temporal and spatial variability, and quantifying the impacts of the important sources in the area.

[3] Volatile organic compounds (VOCs) can directly influence aerosol formation and growth via condensation of semivolatile oxidation products onto existing aerosol surface area [*Odum et al.*, 1996; *Jang et al.*, 2002; *Czoschke et al.*, 2003], and possibly via the homogeneous nucleation of new particles [*Koch et al.*, 2000; *Hoffmann et al.*, 1998]. They also have strong indirect effects on aerosol via their control over ozone production and HO_x cycling, which in turn dictate oxidation rates of organic and inorganic aerosol precursor species. Comprehensive and high time resolution VOC measurements in conjunction with particle measurements thus aid in characterizing chemical conditions con-

[1]Division of Ecosystem Sciences, University of California, Berkeley, California, USA.
[2]Now at Department of Earth and Planetary Sciences, Harvard University, Cambridge, Massachusetts, USA.
[3]Department of Chemical Engineering, Carnegie Mellon University, Pittsburgh, Pennsylvania, USA.
[4]Department of Environmental Sciences, Rutgers University, New Brunswick, New Jersey, USA.
[5]Now at Department of Chemical and Biochemical Engineering, University of Iowa, Iowa City, Iowa,USA.

0148-0227/05/2004JD004601$09.00

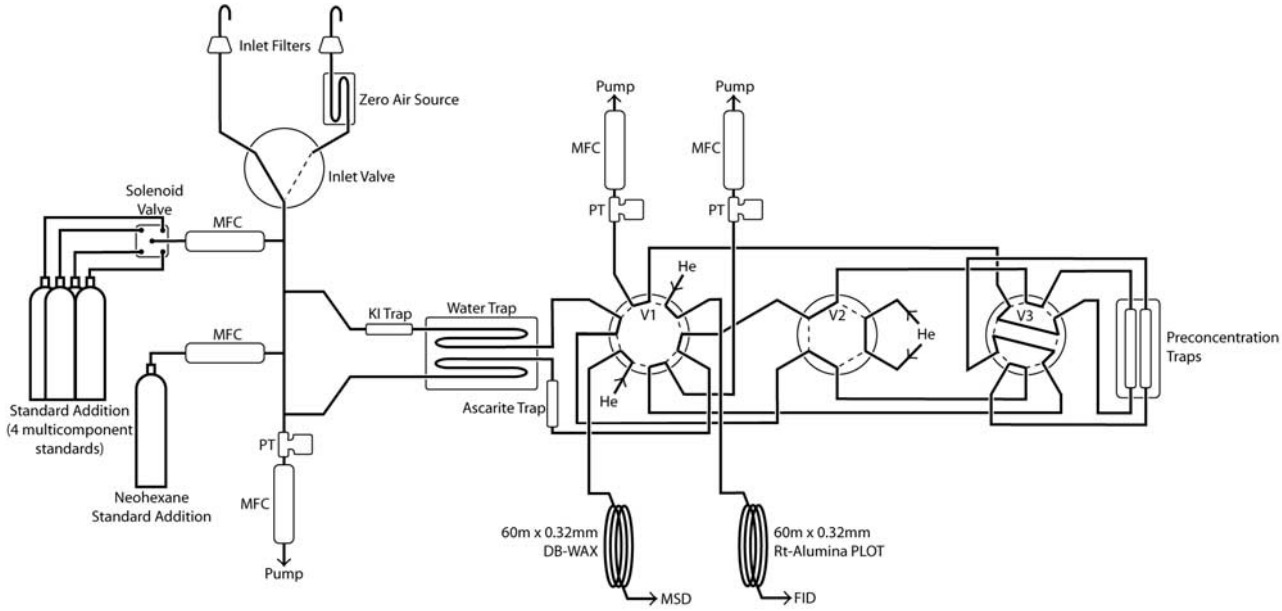

Figure 1. Schematic of the VOC sampling system. MFC, mass-flow controller; V1–V3, valves 1–3; MSD, mass selective detector; FID, flame ionization detector; PT, pressure transducer.

ducive to particle formation and growth. VOC data can also yield information on the nature of source types impacting the study region [*Goldstein and Schade*, 2000], photochemical aging and transport phenomena [*Parrish et al.*, 1992; *McKeen and Liu*, 1993], and estimates of regional emission rates [*Barnes et al.*, 2003; *Bakwin et al.*, 1997], all of which can be useful in interpreting other gas and particle phase measurements.

[4] This paper describes the results from two field deployments, during January–February 2002 and July–August 2002, in which we made in situ VOC measurements alongside the comprehensive aerosol measurements at the PAQS site, with the aim of specifically addressing the connection between atmospheric trace gases and particle formation and source attribution. The data set provides an opportunity to examine aerosol formation and chemistry in the context of high time resolution speciated VOC measurements.

[5] The specific goals of this paper include: characterizing the dominant source types impacting the Pittsburgh region, their composition and variability; assessing the relative importance of different types of VOCs to regional photochemistry, and the relationship between aerosol concentrations and the chemical state of the atmosphere; and quantifying the relative importance of primary and secondary sources in determining organic aerosol and oxygenated VOC (OVOC) concentrations. For the latter we quantify the primary emission ratios for species with multiple source types, by correlation with combustion and photochemical marker compounds.

2. Experimental

2.1. Pittsburgh Air Quality Study (PAQS)

[6] The field component of the Pittsburgh Air Quality Study was carried out from July 2001 through August 2002. Measurement platforms consisted of a main sampling site located in a park about 6 km east of downtown Pittsburgh, as well as a set of satellite sites in the surrounding region. For details on the PAQS study, see *Wittig et al.* [2004a] and the references cited therein. Measurements described here were made at the main sampling site.

2.2. VOC Measurements

[7] A schematic of the VOC measurement setup is shown in Figure 1. To provide information on as wide a range of compounds as possible, two separate measurement channels were used, equipped with different preconditioning systems, preconcentration traps, chromatography columns, and detectors. Channel 1 was designed for preconcentration and separation of C_3–C_6 nonmethane hydrocarbons, including alkanes, alkenes and alkynes, on an Rt-Alumina PLOT column with subsequent detection by FID. Channel 2 was designed for preconcentration and separation of oxygenated, aromatic, and halogenated VOCs, NMHCs larger than C_6, and some other VOCs such as acetonitrile and dimethylsulfide, on a DB-WAX column with subsequent detection by quadropole MSD (HP 5971).

[8] Air samples were drawn at 4 sl/min through a 2 micron Teflon particulate filter and 1/4″ OD Teflon tubing (FEP fluoropolymer, Chemfluor) mounted on top of the laboratory container. Two 15 scc/min subsample flows were drawn from the main sample line, and through pretreatment traps for removal of O_3, H_2O and CO_2. For 30 min out of every hour, the valve array (V1, V2, and V3; valves from Valco Instruments) was switched to sampling mode (Figure 1, as shown) and the subsamples flowed through 0.03″ ID fused silica-lined stainless steel tubing (Silcosteel, Restek Corp) to the sample preconcentration traps where the VOCs were trapped prior to analysis. When sample collection was complete, the preconcentration traps and downstream tubing were purged with a forward flow of UHP helium for 30 s to remove residual air. The valve array was then switched to inject mode, the preconcentration traps heated rapidly to 200°C, and the trapped analytes desorbed into the helium carrier gas and transported to the GC for separation and quantification.

[9] As noninert surfaces are known to cause artifacts and compound losses for unsaturated and oxygenated species, all surfaces contacted by the sampled airstream prior to the valve array were constructed of Teflon (PFA or FEP). All subsequent tubing and fittings, except the internal surfaces of the Valco valves V1, V2, and V3, were Silcosteel. The valve array, including all silcosteel tubing, was housed in a temperature controlled box held at 50°C to prevent compound losses through condensation and adsorption. All flows were controlled using Mass-Flo Controllers (MKS Instruments), and pressures were monitored at various points in the sampling apparatus using pressure transducers (Data Instruments).

[10] In order to reduce the dew point of the sampled airstream, both subsample flows passed through a loop of 1/8″ OD Teflon tubing cooled thermoelectrically to −25°C. Following sample collection, the water trap was heated to 105°C while being purged with a reverse flow of dry zero air to expel the condensed water prior to the next sampling interval. A trap for the removal of carbon dioxide and ozone (Ascarite II, Thomas Scientific) was placed downstream of the water trap in the Rt-Alumina/FID channel. An ozone trap (KI-impregnated glass wool, following *Greenberg et al.* [1994]) was placed upstream of the water trap in the other channel leading to the DB-WAX column and the MSD (Figure 1).

[11] Sample preconcentration was achieved using a combination of thermoelectric cooling and adsorbent trapping. The preconcentration traps consisted of three stages (glass beads/Carbopack B/Carboxen 1000 for the Rt-Alumina/FID channel, glass beads/Carbopack B/Carbosieves SIII for the DB-WAX/MSD channel; all adsorbents from Supelco), held in place by DMCS-treated glass wool (Alltech Associates) in a 9 cm long, 0.04″ ID fused silica-lined stainless steel tube (Restek Corp). A nichrome wire heater was wrapped around the preconcentration traps, and the trap/heater assemblies were housed in a machined aluminum block that was thermoelectrically cooled to −15°C. After sample collection and the helium purge, the preconcentration traps were isolated via V3 (see Figure 1) until the start of the next chromatographic run. The traps were small enough to permit rapid thermal desorption (−15°C to 200°C in 10 s) eliminating the need to cryofocus the samples before chromatographic analysis (following *Lamanna and Goldstein* [1999]). The samples were thus introduced to the individual GC columns, where the components were separated and then detected with the FID or MSD.

[12] Chromatographic separation and detection of the analytes was achieved using an HP 5890 Series II GC. The temperature program for the GC oven was: 35°C for 5 min, 3°C/min to 95°C, 12.5°C/min to 195°C, hold for 6 min. The oven then ramped down to 35°C in preparation for the next run. The carrier gas flow into the MSD was controlled electronically and maintained constant at 1 mL/min. The FID channel carrier gas flow was controlled mechanically by setting the pressure at the column head such that the flow was 4.5 mL/min at an oven temperature of 35°C. The carrier gas for both channels was UHP (99.999%) helium which was further purified of oxygen, moisture and hydrocarbons (traps from Restek Corp.).

[13] Zero air for blank runs and calibration by standard addition was generated by flowing ambient air over a bed of platinum heated to 370°C. This system passes ambient humidity, creating VOC free air in a matrix resembling real air as closely as possible. Zero air was analyzed daily to check for blank problems and contamination for all measured compounds.

[14] Compounds measured on the FID channel were quantified by determining their weighted response relative to a reference compound (see *Goldstein et al.* [1995a] and *Lamanna and Goldstein* [1999] for details). Neohexane (5.15 ppm, certified NIST traceable ±2%; Scott-Marrin Inc.) was employed as the internal standard for the FID channel, and was added by dynamic dilution to the sampling stream. Compound identification was achieved by matching retention times with those of known standards for each compound (Scott Specialty Gases, Inc.).

[15] The MSD was operated in single ion mode (SIM) for optimum sensitivity and selectivity of response. Ion-monitoring windows were timed to coincide with the elution of the compounds of interest. Calibration curves for all of the individual compounds were obtained by dynamic dilution of multicomponent low-ppm level standards (Apel-Riemer Environmental Inc.) into zero air to mimic the range of ambient mixing ratios. A calibration or blank was performed every 6th run.

[16] The system was fully automated for unattended operation in the field. The valve array (V1, V2 and V3) and the preconcentration trap resistance heater circuit were controlled through the GC via auxiliary output circuitry. The PC controlling the GC was also interfaced with a CR10X data logger (Campbell Scientific Inc.), which was triggered at the outset of each analysis run. The inlet valve, the standard addition solenoid valve and the water trap cooling, heating and valve circuitry were switched at the appropriate times during the sampling cycle by a relay module (SDM-CD16AC, Campbell Scientific) controlled by the data logger. Relevant engineering data (time, temperatures, flow rates, pressures, etc.) for each sampling interval were recorded by the CR10X data logger with a AM416 multiplexer (Campbell Scientific Inc.), then uploaded to the PC and stored with the associated chromatographic data. Chromatogram integrations were done using HP Chemstation software. All subsequent data processing and QA/QC was performed using routines created in S-Plus (Insightful Corp.). Instrumental precision, detection limits, and accuracy for each measured compound during this experiment, along with the 0.25, 0.50, and 0.75 quantiles of the data, are given in Table 1.

2.3. Aerosol, Trace Gas, and Meteorological Measurements

[17] Additional measurements which are used in this paper are described briefly below. For a more thorough overview of the gas and particle measurement methods and results from PAQS, the reader is directed to *Wittig et al.* [2004a] and the references cited therein.

[18] Semicontinuous measurements of PM 2.5 (i.e., <2.5 μm diameter) particulate mass were made using a tapering element oscillating microprobe (TEOM) instrument (Model 1400a, Rupprecht & Patashnick Co., Inc.). PM 2.5 nitrate and sulfate were also measured on a semicontinuous basis using Integrated Collection and Vaporization Cell (ICVC) instruments (Rupprecht & Patashnick Co., Inc.)

Table 1. Concentration Quantiles and Figures of Merit for Measured VOCs

Compound	Precision,[a] %	Detection Limit, ppt	Accuracy, %	Winter[b]		Summer[c]	
				Median, ppt	IQR,[d] ppt	Median, ppt	IQR,[d]
Propane	2.5	1.6	7.6	2960	2087–4307	1787	992–3540
Isobutane	2.5	1.2	7.6	668	479–953	323	212–634
Butane	2.5	1.2	7.6	1333	978–1799	632	375–1106
Isopentane	2.5	0.9	7.6	575	448–809	649	409–1139
Pentane	2.5	0.9	7.6	355	279–493	352	213–613
Methylpentanes[e]	2.5	0.8	7.6	268	203–368	276	183–506
Hexane	2.5	0.8	7.6	147	116–199	129	81–231
Propene	2.5	1.5	7.6	214	147–306	219	159–336
t-2-butene	2.5	1.1	7.6	30	19–52	11	8–18
1-butene	2.5	1.1	7.6	57	40–83	62	44–88
2-methylpropene	2.5	1.1	7.6	38	32–51	NQ[f]	NQ[f]
Cyclopentane	2.5	0.9	7.6	53	35–92	47	36–72
c-2-butene	2.5	1.1	7.6	27	18–44	20	15–28
Cyclopentene	2.5	1.0	7.6	NQ[f]	NQ[f]	3	0–8
Propyne	2.5	1.4	7.6	29	22–40	7	5–12
3-methyl-1-butene	2.5	0.9	7.6	6	5–10	19	12–35
t-2-pentene	2.5	0.9	7.6	19	12–33	44	33–62
1-pentene	2.5	0.9	7.6	36	24–56	20	14–32
2-methyl-1-butene	2.5	0.9	7.6	16	11–25	42	22–74
Benzene	4.4	26	10	279	231–355	215	143–405
Perchloroethylene	5.4	0.6	10	18	12–25	22	13–41
Ethylbenzene	5.8	1.6	10	47	34–69	71	44–141
Isoprene	4.3	3.1	10	<DL[g]	<DL[g]	619	153–1475
Methyl-t-butyl ether	4.2	1.7	10	10	7–14	31	19–61
Acetaldehyde	7.2	82	10	538	403–729	1559	1103–2150
Dimethylsulfide	5.6	3.2	10	NQ[f]	NQ[f]	7	5–10
Acetone	4.0	47	10	943	655–1385	4031	3128–4894
Butanal	6.0	28	10	NQ[f]	NQ[f]	91	64–122
Methacrolein	5.6	11	10	<DL[g]	<DL[g]	266	178–366
3-methylfuran	4.2	2.2	10	<DL[g]	<DL[g]	10	6–16
Methanol	8.2	370	11	3760	2347–5773	10717	7122–14601
Methylethylketone	5.1	10	10	215	153–299	559	408–674
Methylene chloride	7.1	22	10	NQ[f]	NQ[f]	79	48–145
Isopropanol	8.9	23	11	131	86–199	235	147–432
Ethanol	13	16	15	989	673–1416	1722	1017–3567
Methylvinylketone	3.5	6.8	10	<DL[g]	<DL[g]	463	273–665
Pentanal	8.3	19	11	NQ[f]	NQ[f]	137	98–193
Acetonitrile	13	38	14	NQ[f]	NQ[f]	131	105–155
Chloroform	3.6	1.2	10	11	10–13	17	13–30
α-pinene	5.9	0.6	10	<DL[g]	<DL[g]	16	10–29
Toluene	2.9	22	10	331	248–494	443	274–902
Hexanal	11	25	13	34	22–52	NQ[f]	NQ[f]
p-xylene	5.8	3.4	10	62	42–95	91	51–173
m-xylene	5.8	5.3	10	113	76–176	163	89–306
o-xylene	5.8	2.4	10	60	41–89	52	29–93

[a]Defined as the relative standard deviation of the calibration fit residuals.
[b]Dates of 9 January to 12 February 2002.
[c]Dates of 9 July to 10 August 2002.
[d]IQR, interquartile range.
[e]The sum of 2-methylpentane and 3-methylpentane, which coelute.
[f]NQ, not quantified, due to inadequate resolution, unavailability of standard or other reason.
[g]<DL, below detection limit.

[*Wittig et al.*, 2004b]. Aerosol number size distributions (0.003–10 μm) were quantified using an array of particle sizing measurements: a nano scanning mobility particle sizer (SMPS) (TSI, Inc., Model 3936N25), standard SMPS (TSI, Inc., Model 3936L10), and Aerodynamic Particle Sizer (APS) (TSI, Inc., Model 3320). Aerosol number size distribution measurements were made semicontinuously throughout the PAQS campaign [*Stanier et al.*, 2004a]. Aerosol organic carbon (OC) and elemental carbon (EC) were quantified in situ throughout the study with 2–4 hour time resolution using a Sunset Labs in situ carbon analyzer (A. Polidori et al., manuscript in preparation, 2005).

[19] O_3, NO, NO_2, CO and SO_2 were measured continuously with commercial gas analyzers (Models 400A, 200A, 300 and 100A, Teledyne Advanced Pollution Instrumentation). Measurements of relevant meteorological parameters (incoming radiation, air temperature, wind speed and direction, precipitation, and relative humidity) were also made continuously throughout the experiment.

3. Results and Discussion

3.1. Meteorological Conditions

[20] Observed wind speed and direction for the two study periods (9 January to 12 February and 9 July to 10 August 2002) are shown as a wind rose plot in Figure 2. Throughout this paper, data collected during the January–February 2002 deployment will be referred to as "winter" data and

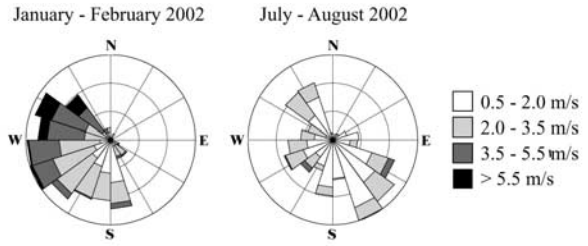

Figure 2. Wind rose plots for the winter and summer experiments. The lengths of the wedges are proportional to the frequency of observation.

that collected during July–August 2002 as "summer" data. Winds in the winter were predominantly out of the west (south to northwest), whereas in the summer southeasterly and northwesterly winds were most common (Figure 2). There was a diurnal cycle in wind speed in both seasons, with stronger winds during the day and weaker winds at night (not shown).

3.2. Factor Analysis

[21] Factor analysis can be used to categorize measured compounds into distinct source groups based on the covariance of their concentrations, creating an understanding of the variety of sources contributing to a broad range of measured species [*Sweet and Vermette*, 1992; *Thunis and Cuvelier*, 2000; *Lamanna and Goldstein*, 1999]. In this section we characterize the dominant source types impacting the Pittsburgh region in summer and winter, based on a factor analysis of the VOC data set, combined with other available trace gas and high temporal resolution aerosol data. Compounds are grouped into factors according to their covariance, and the strength of association between compounds and factors is expressed as a loading matrix. Each factor is a linear combination of the observed variables and in theory represents an underlying process which is causing certain species to behave similarly. Prior knowledge of source types for the dominant compounds is then used to assign source categories to the statistically identified factors.

[22] The analysis was performed using principal components extraction and varimax rotation (S-Plus 6.1, Lucent Technologies Inc.). Species having a significant amount (>8%) of missing data were excluded from the analysis. Results for the winter and summer data sets are presented in Tables 2 and 3, respectively, and discussed in detail below. Compounds not loading significantly on any of the factors are omitted from the loadings tables.

3.2.1. Winter Trace Gas and Aerosol Data Set

[23] Six factors were extracted from the winter data set, which accounted for a total of 83% of the cumulative variance (Table 2). Each of the six factors accounted for a statistically significant portion of the variance ($P < 0.01$, where P is the statistical probability of incorrectly attributing a nonzero fraction of the variance to a given factor). The analysis was limited to six factors since including more factors failed to account for more than an additional 2% of the variance in the data set.

[24] Factor 1, explaining 44% of the total variability in the data set, was associated most strongly with short-lived combustion-derived pollutants, such as the anthropogenic alkenes and aromatic species, in addition to NO_x and the gasoline additive methyl-t-butyl ether (MTBE). We attribute this factor to local automobile emissions. The diurnal cycle exhibited by this factor (Figure 3a) showed a clear pattern, higher during the day than at night, and with prominent peaks during the morning and evening rush hours. Note that factor 1 accounted for 44% of the data set variability, indicating that automobile exhaust was most strongly responsible for changes in atmospheric VOC concentrations in Pittsburgh in the winter. Note also, however, that none of the aerosol parameters included in the factor analysis (PM 2.5 mass, aerosol sulfate and nitrate mass, and aerosol number density) loaded significantly on this factor, suggesting that this source was a relatively minor contributor to these components of regional PM.

[25] Factor 2, accounting for 10% of the variance, was associated exclusively with the anthropogenic alkanes (Table 2), most strongly with propane, and probably represents leaks of propane fuel or natural gas. None of the aerosol measurements loaded on this factor. Factor 2 was on average highest with winds out of the south, and the diurnal pattern showed a maximum in the early morning before dawn (Figure 3b), with a minimum in the afternoon.

[26] The third factor, accounting for 9% of the data set variance, like factor 1 was associated with some gas-phase combustion products (such as CO, benzene and propyne). Unlike factor 1, however, it also contained a significant aerosol component, in particular sulfate and PM 2.5 mass. The diurnal cycle of factor 3 (Figure 3c) was distinct from that of factor 1, with higher concentrations at night, and no noticeable rush hour contribution. The highest levels of factor 3 were seen with winds out of the south-southeast. We attribute this factor to industrial emissions from point sources in the region. In particular, the U.S. Steel Clairton Works, which is the largest manufacturer of coke and coal chemicals in the United States, and is located 11 miles to the south-southeast of Pittsburgh, may have been a significant contributor to this factor.

[27] Factor 4 was composed of species (acetone, acetaldehyde, methylethylketone (MEK)) that are both emitted directly and produced photochemically. Acetone and acetaldehyde are also known to have significant biogenic sources [*Schade and Goldstein*, 2001]; however, biogenic emissions are unlikely to be a dominant source of these compounds in the Pittsburgh winter. PM 2.5 mass was also associated with this category, consistent with the importance of both primary emissions and secondary production of regional aerosol. The diurnal cycle of factor 4 (Figure 3d) showed evidence of both primary and secondary influence. Daytime concentrations were slightly higher than at night, and there was a marked increase in the morning which was coincident with sunrise. Unlike factor 1, this factor did not show the distinct morning and evening peaks coinciding with rush hour. The day-night difference was much less than in summer (see following section), likely reflecting weak wintertime photochemistry and a consequently greater relative impact from direct emissions. The relative importance of primary and photochemical sources for these compounds is explored further in section 3.3.

[28] Factor 5, which explained a further 6% of the variance, was negatively associated with ozone and nuclei mode aerosol number density, and positively associated with total PM 2.5 mass, aerosol nitrate and accumulation

Table 2. Factor Analysis Results: Winter Data[a]

	Loadings					
Compound	Factor 1: Local Auto	Factor 2: Natural Gas	Factor 3: Industrial	Factor 4: 1° + 2°	Factor 5: 2° + Mix	Factor 6: Coal
Propane		0.87				
Isobutane	0.64	0.66				
Butane	0.63	0.63				
t-2-butene	0.90					
Isopentane	0.76	0.49				
Pentane	0.63	0.62				
Methylpentanes[b]	0.77	0.44				
Hexane	0.65	0.54				
Propene	0.76		0.47			
1-butene	0.86					
2-methylpropene	0.60		0.49			
Cyclopentane	0.57					
c-2-butene	0.91					
Propyne	0.64		0.53			
3-methyl-1-butene	0.90					
t-2-pentene	0.90					
1-pentene	0.91					
2-methyl-1-butene	0.91					
Benzene	0.42		0.63			
C_2Cl_4	0.68					
Ethylbenzene	0.89					
MTBE	0.74					
Acetaldehyde	0.41			0.58		
Acetone				0.82		
MEK	0.47			0.64		
Chloroform	0.52					
Toluene	0.80					
Hexanal	0.61					
p-xylene	0.90					
m-xylene	0.91					
o-xylene	0.90					
O_3					−0.68	
NO_x	0.76					
SO_2						0.75
CO	0.52		0.59			
PM 2.5			0.50	0.42	0.44	0.40
Aerosol SO_4^{2-}			0.54			0.54
Aerosol NO_3^-					0.62	
N_{nuc}[c]					−0.42	
N_{acc}[c]			0.41		0.45	0.59
Importance of factors						
Fraction of variance	0.44	0.10	0.09	0.08	0.06	0.06
Cumulative variance	0.44	0.54	0.63	0.71	0.77	0.83

[a]The degree of association between measured compounds and each of the six factors is indicated by a loading value, with the maximum loading being 1. Loadings of magnitude <0.4 omitted.

[b]The sum of 2-methylpentane and 3-methylpentane, which coelute.

[c]N_{nuc} and N_{acc} refer to aerosol number densities in the nuclei (3–10 nm) and accumulation (100–500 nm) modes.

mode number density. This factor may represent the combined influences of photochemical activity and mixed layer dynamics. Production of ozone and nucleation mode particles is driven by sunlight, and owing to their relatively short lifetimes their concentrations were highest during the day and lower at night. By contrast, longer lived pollutants less strongly impacted by photochemistry exhibited higher concentrations at night when winds were calmer and vertical mixing limited. In addition, partitioning of semivolatile species such as nitrate into the particle phase is thermodynamically favored by the colder temperatures and higher relative humidity at night.

[29] The 6th factor, accounting for 6% of the variability, was associated with gas phase SO_2, aerosol sulfate, PM 2.5 mass, and accumulation mode number density. Factor 6 showed a diurnal pattern with higher impact during the day than at night, consistent with a photochemically driven process (Figure 3f). However, nucleation mode number density did not load significantly on this factor. This factor may reflect regional coal burning power plant emissions of gases and particles, and the subsequent photochemical aging of those emissions.

3.2.2. Summer Trace Gas and Aerosol Data Set

[30] Six factors were extracted from the summer data set, which together accounted for 77% of the variability in the observations (Table 3). Each of the six factors accounted for a statistically significant portion of the variance ($P < 0.01$). Including additional factors explained less than 2% of the remaining variance. The PM 2.5 measurements had a large number (19%) of missing values, and as there was a strong correlation ($r^2 = 0.92$) between PM 2.5 mass and aerosol volume measured with the SMPS, missing PM 2.5 concentrations were estimated by scaling to aerosol volume prior to performing the factor analysis.

Table 3. Factor Analysis Results: Summer Data[a]

	Loadings					
Compound	Factor 1: Local Auto	Factor 2: 2° + Bio	Factor 3: Transport	Factor 4: Industrial	Factor 5: Isopentane Ox	Factor 6: Natural Gas
Propane	0.59					0.58
Isobutane	0.74					0.54
Butane	0.78					0.52
Isopentane	0.91					
Pentane	0.89					
Methylpentanes[b]	0.93					
Hexane	0.90					
Propene	0.71			0.45		
t-2-butene	0.89					
1-butene	0.57	0.66				
Cyclopentane	0.66			0.49		
c-2-butene	0.80					
Propyne	0.88					
3-methyl-1-butene	0.95					
t-2-pentene	0.94					
1-pentene	0.93					
2-methyl-1-butene	0.82					
Benzene				0.68		
C_2Cl_4	0.48					
Ethylbenzene	0.89					
Isoprene		0.44				
MTBE	0.91					
Acetaldehyde		0.88				
Acetone		0.64	0.64			
Butanal		0.85				
MACR					0.90	
3-methylfuran		0.45			0.53	
MEK	0.44	0.44	0.40			
Isopropanol	0.47					
MVK					0.89	
Pentanal	0.55	0.72				
Acetonitrile				0.43		
Chloroform	0.67					
α-pinene	0.57					
Toluene	0.80			0.47		
p-xylene	0.90					
m-xylene	0.90					
o-xylene	0.84					
O_3	−0.51					−0.43
NO_x	0.52			0.44		
SO_2			0.42			
CO	0.50			0.44		
PM 2.5			0.88			
Aerosol SO_4^{2-}			0.85			
N_{acc}[c]			0.70			
Importance of factors						
Fraction of variance	0.42	0.10	0.08	0.07	0.05	0.04
Cumulative variance	0.42	0.53	0.60	0.67	0.73	0.77

[a]The degree of association between measured compounds and each of the six factors is indicated by a loading value, with the maximum loading being 1. Loadings of magnitude <0.4 omitted.
[b]The sum of 2-methylpentane and 3-methylpentane, which coelute.
[c]Accumulation mode (100–500 nm) aerosol number density.

[31] As with the winter data, the dominant factor, explaining 42% of the total variance, was associated with anthropogenic alkenes, aromatics, MTBE and other markers of tailpipe emissions (Table 3). The diurnal cycle of this source type (Figure 4a), however, with a sharp early morning maximum at sunrise and a broad afternoon minimum, was markedly different than in the winter, when traffic patterns determined the diurnal pattern. In summer, a deeper daytime mixed layer and more rapid photooxidation combined to give rise to the observed temporal pattern. The fact that benzene is not associated with factor 1 is due to the influence of a nearby source (not associated with other tailpipe compounds or solvents), which resulted occasionally in extremely elevated benzene levels. If the factor analysis is repeated after removing the highest (>0.9 quantile) benzene values, benzene in fact loads most strongly on this automotive factor.

[32] Factor 2 encompassed compounds, such as acetone, acetaldehyde, and isoprene, known to have photochemical sources, sunlight dependent biogenic sources, or both. We thus interpret this factor as representing a combination of these radiation-driven source types. The clear diurnal pattern for this source category (Figure 4b) reflected its light dependent nature, and suggests, for the associated OVOCs, that photochemical and/or biogenic production were more important than direct combustion emissions. The association of 1-butene with factor 2 suggests a regional light-driven biogenic 1-butene source, as has been reported for other locations [*Goldstein et al.*, 1996].

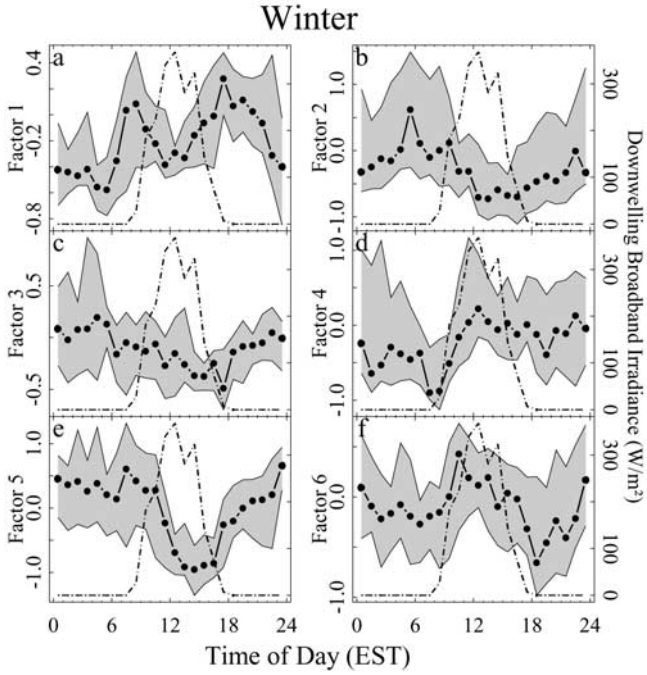

Figure 3. Median diurnal cycles in factor scores (circles) for the winter data set. Banded gray areas show the interquartile range. Incoming solar radiation is also shown (dot-dash line).

[33] Factor 3, consisting of fine particle number (accumulation mode only; nuclei and aitken mode number densities were not included in the analysis as they contained too many missing values), PM 2.5 mass, sulfur dioxide, and particle sulfate, had a weak diurnal pattern containing a maximum at midday (Figure 4c). The correlation of acetone and MEK with the other species associated with this factor may arise from distinct sources which lie along the same transport trajectory, or may reflect long-range transport of pollution with concurrent photochemical production.

[34] The fourth factor, which explained 7% of the cumulative variance, associated with combustion markers such as benzene, NO_x and CO, is analogous to the source represented by the third factor extracted from the winter data set. The two factors both exhibited diurnal patterns with concentrations elevated at night and early morning (Figures 3c and 4d), and in both cases the highest levels were associated with winds from the south-southeast. Again, we attribute this factor to industrial emissions. PM 2.5 loaded on the analogous factor in the winter data set, but was not significantly associated with this factor in the summer. This may be due to the fact that concentrations of all measured PM components increased significantly during the summer, and so the contribution of this local source to the total PM 2.5 mass was less important during this time. The fifth factor accounted for a further 5% of the data set variance and was associated exclusively with oxidation products of isoprene: methacrolein (MACR), methylvinylketone (MVK) and 3-methylfuran.

[35] Propane, isobutane and butane grouped together on factor 6, which likely represents propane fuel or natural gas leakage. The diurnal pattern for this factor (Figure 4f) was similar to that of factor 1, with a strong predawn maximum and afternoon minimum. There was also a weak negative association with ozone, as there was with factor 1, owing to the co-occurrence of the maximum mixed layer depth (and lowest levels of factor 1 and factor 6 compounds) with the maximum daily ozone concentrations.

3.2.3. Summary of Factor Analysis Results

[36] The results of the factor analyses provide a context from which to interpret the combined VOC and fine particle data sets. In both seasons, local tailpipe emissions formed a substantial component of the ambient VOC concentrations. They did not, however, significantly impact the aerosol species that were included in the factor analysis. Nonautomotive combustion emissions, probably from industrial point sources in the area, were an important source of aerosol mass, as well as of CO, NO_x and several unsaturated hydrocarbons. There was pronounced photochemical production of OVOCs such as acetone, MEK, and acetaldehyde in summer. Diurnal concentration patterns indicated that this source was more important than primary combustion emissions. In winter this was not the case, although secondary production was still evident. Along with isoprene, 1-butene showed evidence of a local light-driven biogenic source. There was a distinct source of alkanes that did not appear to be a significant source of other compounds, which was likely leakage of propane fuel or natural gas. Finally, ambient PM showed evidence of a significant secondary component even in winter. The importance of primary and secondary sources to OVOC and OC levels is explored in detail in the following section.

3.3. Source Apportionment of OVOCs and Aerosol Organic Carbon

3.3.1. OVOC Source Apportionment

[37] Oxygenated VOCs can make up a sizable and even dominant fraction of the total VOC abundance and reactiv-

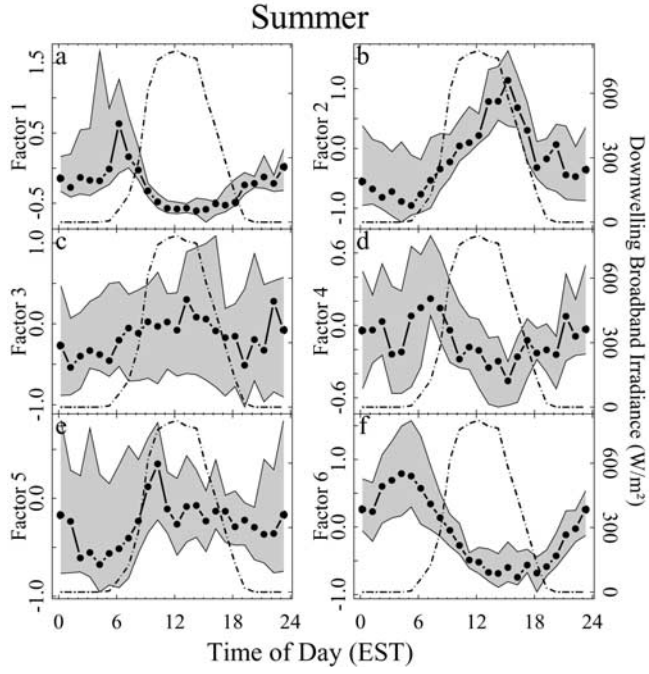

Figure 4. Median diurnal cycles in factor scores (circles) for the summer data set. Banded gray areas show the interquartile range. Incoming solar radiation is also shown (dot-dash line).

ity, in the urban [*Grosjean*, 1982; *Goldan et al.*, 1995a], rural [*Goldan et al.*, 1995b; *Riemer et al.*, 1998], and even remote marine atmosphere [*Singh et al.*, 1995, 2001]. Many OVOCs, such as acetone, MEK and acetaldehyde, are known to have a diversity of sources, including combustion emissions, photochemical production from both anthropogenic and biogenic precursor species, and direct biogenic emissions. Understanding the magnitudes of these sources in different environments is prerequisite to an accurate representation of odd hydrogen cycling and ozone chemistry in models of atmospheric chemistry and air quality from the local to global scale.

[38] Here we present a new approach to unraveling source contributions to such species. We define the ambient concentrations of VOC species Y (χ_y, in ppt) as being the sum of direct combustion (χ_{yc}) and other components (χ_{yo}), which could represent secondary or biogenic sources, as well as a background concentration (χ_a),

$$\chi_y = \chi_{yc} + \chi_{yo} + \chi_a. \quad (1)$$

[39] For relatively long lived species, such as acetone, χ_a may be considered to represent a regional background level. In this case, χ_a will presumably include contributions from both combustion and secondary/biogenic production that has taken place elsewhere and been integrated into the regional background. For acetaldehyde, a compound with an atmospheric lifetime of only a few hours, there was nonetheless a nonzero observed minimum concentration in both summer and winter. Here, the parameter χ_a may represent a relatively invariant area source that maintains ambient levels of acetaldehyde above a certain threshold. In either case, we operationally define the background concentration of each species as the 0.1 quantile of the measured concentrations [*Goldstein et al.*, 1995b].

[40] If Y and a combustion tracer, such as toluene, are emitted in a relatively consistent ratio from different types of combustion sources, then χ_{yc} can be estimated as

$$\chi_{yc} = \chi_{tol}\left(\frac{Y}{TOL}\right)_E, \quad (2)$$

where $(Y/TOL)_E$ is the primary emission ratio of Y relative to toluene, and χ_{tol} represents toluene enhancements above background (ppt; see the following section for a discussion of the choice of combustion marker). χ_{yo} is then given by

$$\chi_{yo} = \chi_y - \chi_{tol}\left(\frac{Y}{TOL}\right)_E - \chi_a. \quad (3)$$

In (3), χ_{tol}, χ_y, and χ_a are known quantities. All that is required to calculate the combustion (χ_{yc}) and secondary plus biogenic (χ_{yo}) components of species Y is the primary emission ration $(Y/TOL)_E$.

[41] To determine $(Y/TOL)_E$ for each species Y, we make use of the combustion tracers associated with the first factor in the factor analyses (Tables 2 and 3). For a given value of $(Y/TOL)_E$, we can calculate a χ_{yo} vector, and the coefficient of determination (r^2) between χ_{yo} and each of our combustion tracers. By varying $(Y/TOL)_E$ over a range of possible values and repeating this calculation, we can derive r^2 between the calculated χ_{yo} and each of our combustion tracers, as a function of $(Y/TOL)_E$. At low values of $(Y/TOL)_E$, the calculated χ_{yo} will still contain a significant combustion component. At high values of $(Y/TOL)_E$, χ_{yo} will become dominated by the χ_{tol} term. At the correct value for $(Y/TOL)_E$ all contributions of combustion emissions should be removed from χ_{yo}, and hence correlation of χ_{yo} with a pure combustion parameter should be at a minimum. Conversely, if the noncombustion sources of Y are dominantly photochemical, then the correlation between χ_{yo} and a photochemically derived VOC should reach a maximum at that same point.

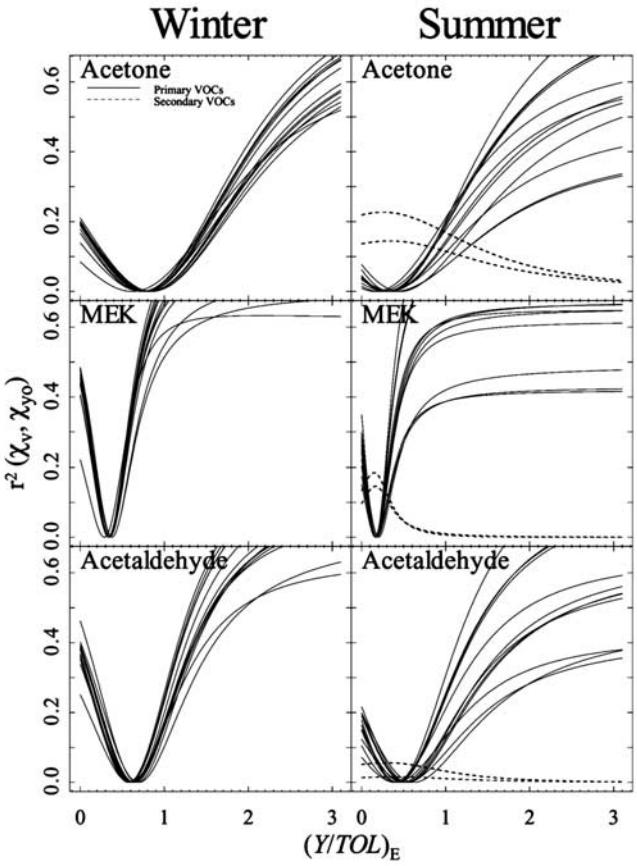

Figure 5. Coefficient of determination between combustion or photochemically derived VOCs and the residual term χ_{yo}, representing photochemical and biogenic OVOC sources, as a function of the primary emission ratio $(Y/TOL)_E$. Each solid (dashed) line represents a separate combustion (photochemical) marker compound (V, with mixing ratio χ_v, for V = propyne, 2-methylpropene, t-2-butene, c-2-butene, 2-methyl-1-butene, 3-methyl-1-butene, t-2-pentene, benzene, ethylbenzene, p-xylene, m-xylene, o-xylene, NO_x, MACR, or MVK). The critical point in the curves gives the combustion emission ratio for species Y (acetone, MEK, or acetaldehyde) relative to toluene.

[42] The results of performing this analysis for Y = acetone, MEK and acetaldehyde are shown in Figure 5. Each solid line shows the coefficient of determination between an individual combustion marker and χ_{yo}, as a function of the value of $(Y/TOL)_E$ that was used to calculate χ_{yo}. The compounds used as markers of combustion (V, with mixing ratios χ_v) were those VOCs thought to

Table 4. OVOC Combustion Emission Ratios and Source Contributions[a]

	Ambient Concentration		Primary Emission Ratio		Background Concentration			Combustion Emissions				Other Sources			
	χ_y, ppt		$(Y/TOL)_E$		χ_a,	χ_a/χ_y		χ_{yc}, ppt		χ_{yc}/χ_y		χ_{yo}, ppt		χ_{yo}/χ_y	
Species (Y)	Median	IQR[b]	Median	IQR[b]	ppt	Median	IQR[b]	Median	IQR[b]	Median	IQR[b]	Median	IQR[b]	Median	IQR[b]
Winter															
Acetone	943	655–1390	0.78	0.74–0.82	526	0.56	0.38–0.80	114	49–241	0.12	0.05–0.21	237	23–624	0.24	0.04–0.48
MEK	215	153–299	0.34	0.34–0.34	120	0.56	0.40–0.79	50	21–105	0.23	0.10–0.39	24	0–92	0.12	0.00–0.35
Acetaldehyde	538	403–729	0.62	0.60–0.64	289	0.54	0.40–0.72	91	39–192	0.17	0.07–0.31	146	24–290	0.27	0.05–0.40
Summer															
Acetone	4030	3130–4890	0.32	0.29–0.34	2650	0.66	0.54–0.85	81	29–224	0.02	0.01–0.06	1200	353–1940	0.29	0.12–0.41
MEK	559	408–674	0.17	0.16–0.18	319	0.57	0.47–0.78	45	16–123	0.10	0.03–0.23	138	29–257	0.26	0.06–0.40
Acetaldehyde	1560	1100–2150	0.43	0.40–0.52	798	0.51	0.37–0.72	113	40–310	0.09	0.03–0.20	542	126–1050	0.34	0.11–0.50

[a]Note that the median values of the source contributions do not necessarily add up to the median ambient concentration as the median is not a distributive property.
[b]IQR, interquartile range.

be solely or predominantly derived via combustion processes (propyne, 2-methylpropene, t-2-butene, c-2-butene, 2-methyl-1-butene, 3-methyl-1-butene, t-2-pentene, benzene, ethylbenzene, p-xylene, m-xylene, o-xylene) and NO_x. Dashed lines show r^2 between χ_{yo} and VOCs thought to be solely photochemically produced (MACR and MVK, which were present above detection limit in the summer experiment only), as a function of $(Y/TOL)_E$.

[43] There is a well defined minimum in the curve for the combustion markers, the location of which, for a given oxygenated VOC species Y, is consistent across all marker compounds. For the summer data, the location of this minimum coincides with the maximum r^2 value for the photochemically produced tracer species. We interpret the location of the critical value of r^2 as the representative $(Y/TOL)_E$ value for that time of year (Table 4).

[44] Primary emission ratios, relative to toluene, for acetone, MEK and acetaldehyde were all substantially (1.4–2.4 times) higher in January–February 2002 than in July–August 2002. Since the emission ratio depends on the toluene as well as OVOC emission strength, seasonal changes in the emission ratio can be due to changes in the numerator, denominator or both. This issue is discussed further in the following section. The primary emission ratios calculated in this section are averages over the sources impacting the air masses that were sampled during the course of the study. They therefore represent integrated regional emission ratios for Pittsburgh in January–February and July–August 2002.

[45] Urban and industrial VOC emission ratios depend on a number of factors, in particular vehicle fleet and fuel characteristics as well as types of industrial activity in the region. Such variability complicates efforts to construct reliable emission inventories for use in air quality modeling, and emphasizes the utility of the approach developed here, which provides top-down observational constraints on regional pollutant emission ratios. On-road studies of motor vehicle exhaust in the U.S. (generally carried out during summer) report emission ratios for acetone, MEK and acetaldehyde relative to toluene ranging from 2–4%, 2–12%, and <1–8% (molar basis) respectively for light-duty vehicles [*Kirchstetter et al.*, 1999; *Fraser et al.*, 1998; *Zielinska et al.*, 1996; *Kirchstetter et al.*, 1996]. Heavy-duty or diesel vehicles emit substantially higher amounts of these OVOCs relative to toluene, with emission ratios frequently greater than unity [*Zielinska et al.*, 1996; *Staehelin et al.*, 1998]. Inventory estimates (including mobile, point and nonpoint sources) of annual acetaldehyde and MEK emissions in Allegheny County are 14% and 10% those of toluene respectively on a molar basis (see http://www.epa.gov/ttn/chief/net/index.html), substantially lower than the values determined here (Table 4). If inventory estimates of toluene emissions are accurate, this suggests that acetaldehyde and MEK emissions are underestimated by factors of approximately 3.8 and 2.6 (from the average of the summer and winter ratios, Table 4).

[46] For the summer data, χ_{yo} for both acetone and MEK exhibited a well-defined maximum correlation with MACR and MVK (Figure 5), indicating that the other, noncombustive, source represented by χ_{yo} is likely to be largely photochemical. For acetaldehyde, the poor correlation of χ_{yo} with MACR and MVK suggests that χ_{yo} is not exclusively photochemical in nature, and may contain another significant component such as biogenic emissions.

[47] For comparison, Figure 6 shows results of the same analysis for Y = MACR and MVK, species whose only significant known source is from photochemical oxidation of isoprene. In this case, the minimum correlation of χ_{yo} with combustion derived VOCs (and maximum correlation with MVK or MACR) occurs at a combustion emission ratio $(Y/TOL)_E$ of zero, showing that there are no significant primary emissions of these compounds.

[48] With $(Y/TOL)_E$ determined by the critical points in Figure 5, the contributions to the concentration of species Y from background (χ_a), combustion emissions (χ_{yc}), and other sources (χ_{yo}) as a function of time can then be calculated from (2) and (3). Contributions of χ_a, χ_{yc}, and χ_{yo} to the ambient levels of acetone, MEK, and acetaldehyde in summer and winter are summarized in Table 4. Negative values of χ_{yo} were assumed to contain no secondary or biogenic material and were set to zero.

[49] Ambient concentrations of acetone, MEK and acetaldehyde during summer were on average 3–4 times higher than winter (Table 4). Increases in background concentrations were responsible for a significant portion of this winter to summer difference, with summer background levels on average 2.5–5 times higher than in the winter. However, the fraction of the total concentration due to the background was comparable in summer and winter. In both seasons, the background made up, on average, slightly over half of the

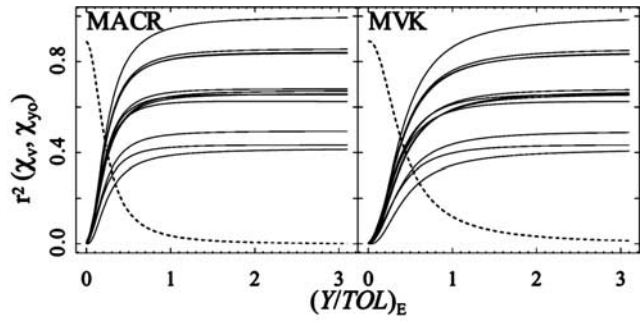

Figure 6. Same as Figure 5, except for Y = methacrolein (MACR) and methylvinylketone (MVK). The minimum correlation of χ_{yo} with combustion derived VOCs (and maximum correlation with photochemical VOCs) occurs at an emission ratio $(Y/TOL)_E$ of zero, showing that there are no significant primary emissions of these compounds.

overall abundance for all three compounds (Table 4). The higher summer background concentrations for these species were probably due to increased nonlocal photochemical production and biogenic emission during that time of year.

[50] The absolute contribution from combustion to atmospheric mixing ratios was very similar in summer and winter, despite the large changes in emission ratios (which were higher in winter by factors of 2.4, 2.0 and 1.4 for acetone, MEK and acetaldehyde; see discussion in following section). However, total concentrations were substantially higher in summer, and combustion emissions were a significantly smaller fraction of the total source (Table 4).

[51] Other sources, which we assume to be predominantly photochemical but which also likely include some biogenic emissions in summer, were substantially higher in summer for all three compounds. Median summer values of χ_{yo} were over 5 times higher than in winter for acetone and MEK and nearly 4 times higher for acetaldehyde.

[52] With the exception of MEK, combustion was not the major source of these compounds, even in winter. For MEK, combustion emissions were more important than other sources (χ_{yo}) in the winter (a median of 23% versus 13%). This was not the case in the summer, however, nor was it true for acetone or acetaldehyde in either season. For acetone, other sources were twice as important as combustion emissions in the winter and ten times as important in the summer. For acetaldehyde, other sources were 50% larger than combustion emissions in winter and 4 times larger in summer.

[53] Diurnally averaged OVOC source contributions, overlaid with ozone concentrations, in winter and summer are shown in Figure 7. For the summer data set, the other OVOC sources (χ_{yo}) showed a strong photochemical signature: low at night, increasing after sunrise and peaking in the afternoon. For each compound, acetone, MEK and acetaldehyde, the χ_{yo} term tracked ozone quite closely. For the winter data set, the χ_{yo} terms for each OVOC showed a much weaker photochemical signal, and the relative contribution from combustion was substantially larger than in the summer. Note that since χ_{yc} for each

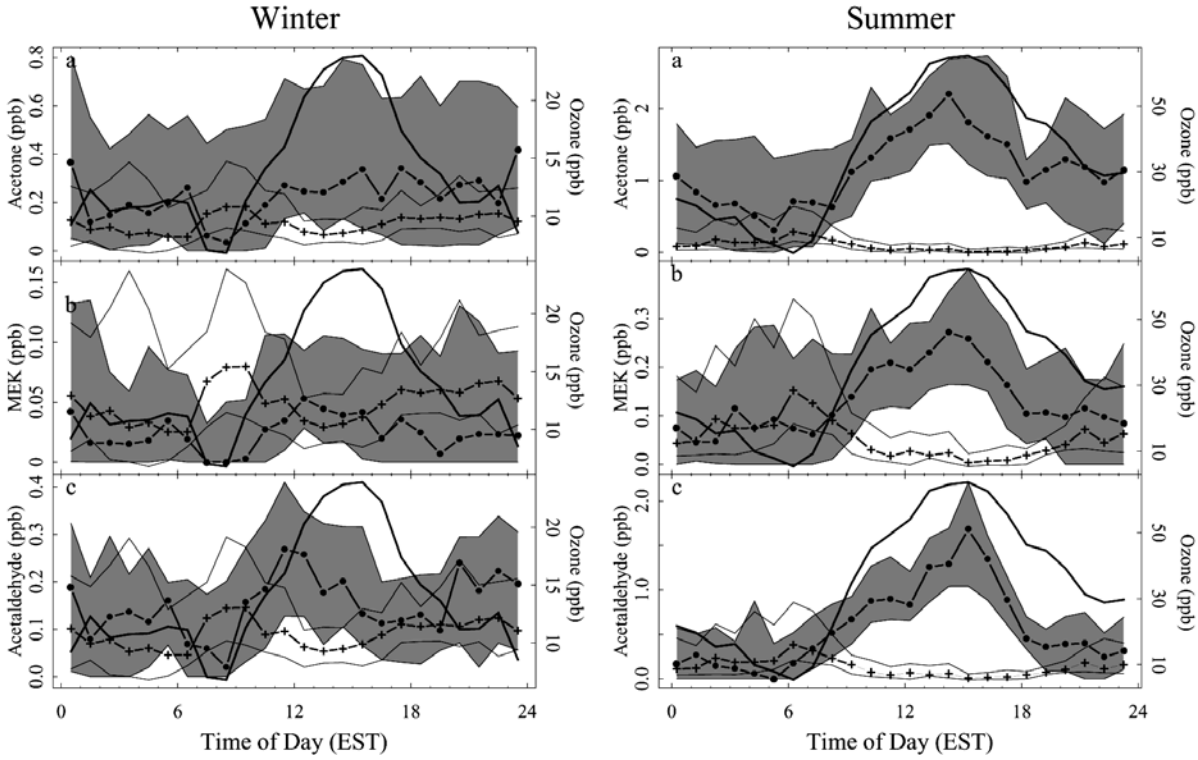

Figure 7. Diurnal patterns in OVOC source contributions (winter and summer data). Combustion source (χ_{yc}, ppb), pluses and unshaded region; photochemical and biogenic sources (χ_{yo}, ppb), circles and surrounding gray area. Ozone is also shown (solid dark line). Points show median values; banded areas show the interquartile range. Note different *y* axis scales for winter and summer.

OVOC is defined as $\chi_{tol}(Y/TOL)_E$, i.e. the observed toluene enhancements multiplied by a primary emission ratio, diurnal patterns in χ_{yc} shown in Figure 7 reflect that of toluene.

3.3.2. Choice of Combustion Marker and Seasonal Patterns in Emission Ratios

[54] Repeating the above analysis using other combustion derived compounds instead of toluene as the primary emission tracer resulted in only minor changes to the calculated OVOC partitioning (Table 4) and did not alter any of the conclusions. This gives us confidence that this approach to partitioning VOC source contributions is robust. For a given primary emission tracer, the calculated OVOC emission ratios, given by the critical r^2, were consistent using compounds that are solely combustion derived (e.g. alkenes and alkynes) and compounds that have additional anthropogenic noncombustion sources, such as evaporative losses and chemical processing (e.g. benzene and toluene). Hence the approach is not sensitive to slight differences in source profiles for the marker compounds. We conclude that the calculated emission ratios represent an integrated regional primary pollution signal, rather than one specific source type.

[55] In addition, we note that the combustion markers employed to calculate the OVOC primary emission ratios relative to toluene (Figure 5) have lifetimes that vary by nearly a factor of 50, yet they give consistent emission ratio estimates. This may indicate that much of the variability observed is relatively local and not driven by photochemical lifetime or by the different sampling footprints for species of different lifetimes.

[56] Seasonal differences in the OVOC primary emission ratios, however, calculated relative to the tracer compound, changed dramatically depending on the tracer used. This is to be expected since the primary emission ratios are sensitive to changes in both the numerator and denominator, and different combustion tracers do not necessarily have identical seasonal patterns in emission strength. While the primary OVOC emission ratios relative to toluene were all higher in the winter, OVOC emission ratios calculated relative to alkenes and alkynes were generally 2–3 times higher in the summer. It is possible that noncombustion toluene sources, i.e. evaporative emissions, are higher in summer which would decrease the OVOC emission ratio for that time of year. However, the short-lived alkenes are oxidized much more rapidly in the summer months due to higher concentrations of OH and ozone. Over a given source-receptor distance, then, the alkenes would be more depleted relative to the OVOCs in the summer than in the winter. This would lead to higher OVOC:alkene emission ratios in the summer, as observed. While this effect would also occur with toluene, either the effect was small due to toluene's longer lifetime (10 times that of t-2-butene) and/or it was offset by increased emissions.

3.3.3. Quantification of Secondary Organic Aerosol

[57] Organic carbon (OC) constitutes a significant fraction of atmospheric aerosol [*Lim and Turpin*, 2002; *Cabada et al.*, 2002, 2004; *Tolocka et al.*, 2001]; however, its origin and composition remain poorly understood. OC consists of hundreds or thousands of individual organic compounds. Both anthropogenic sources (e.g. combustion) and biogenic sources (e.g. plants) can contribute to aerosol organic carbon via direct emission of particles (primary OC), and via emission of gas-phase precursor compounds that partition into the aerosol phase upon oxidation (secondary OC). Clarifying the roles of primary and secondary OC production is an important step toward an improved understanding and modeling of the sources, morphology and effects of aerosol OC. The technique of minimizing (maximizing) the correlation between combustion (photochemical) tracer compounds and the photochemical component of a species of interest, developed in the previous section, also has utility in determining the primary emission ratio for pollutants other than VOCs. Here, we apply the method to quantify the relative importance of primary and secondary OC sources in the study region.

[58] As above, aerosol organic carbon concentrations (M_{oc}, in μg of carbon per cubic meter, $\mu gC/m^3$) are defined as being composed of combustion (M_c) and other (M_o) components, plus a regional background (M_a) [*Turpin and Huntzicker*, 1995]:

$$M_{oc} = M_c + M_o + M_a. \tag{4}$$

[59] Elemental carbon (EC, or soot) is an aerosol component whose only source is direct emission from combustion. If both OC and EC are emitted from primary sources according to a characteristic averaged OC:EC emission ratio $(OC/EC)_E$, then the combustion-derived organic carbon can be estimated as

$$M_c = M_{ec}\left(\frac{OC}{EC}\right)_E, \tag{5}$$

where M_{ec} represents elemental carbon enhancements above background (in $\mu gC/m^3$), and M_o is given by

$$M_o = M_{oc} - M_{ec}\left(\frac{OC}{EC}\right)_E - M_a. \tag{6}$$

[60] The background term, M_a, represents noncombustion primary OC (e.g. from biogenic sources) as well as any regional aerosol organic carbon background. As above, we estimate M_a as the 0.1 quantile of the measured OC concentrations. M_o is then assumed to be exclusively secondary OC. It should be pointed out, however, that if there exist significant sources of primary OC which do not correlate with EC and are highly variable through time (and thus are not entirely captured by the M_a parameter), then M_o may also contain some primary influence.

[61] One challenge associated with the EC tracer method as it has been applied in the past involves defining the OC:EC ratio of primary emissions, as this can vary significantly between sources and consequently as a function of time. In addition, defining $(OC/EC)_E$ from ambient OC and EC concentration data requires that there be a subset of data with no significant secondary contributions to the measured OC concentrations. The typical approach is to qualitatively eliminate data points that are likely to be impacted by significant secondary production or other factors such as rain events, and regress OC on EC for that subset of data dominated by primary OC [*Turpin and Huntzicker*, 1995; *Cabada et al.*, 2004]. This then gives a regression slope that is in theory reflective solely of primary emissions. The

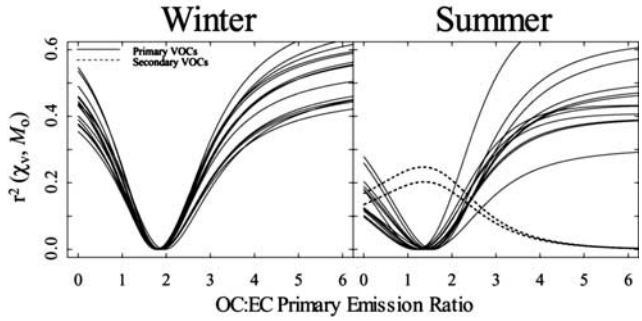

Figure 8. Coefficient of determination between combustion or photochemically derived VOCs and the residual term M_o, representing secondary OC, as a function of the primary emission ratio $(OC/EC)_E$. Each solid (dashed) line represents a separate combustion (photochemical) marker compound. The critical point in the curves gives the primary emission ratio $(OC/EC)_E$.

parameter M_a, reflecting primary noncombustion OC, is then assumed to be constant and given by the intercept, enabling the calculation of M_o. In the event of significant temporal variability in the primary OC:EC ratio impacting the sampling site, this process may be repeated on subsets of the data.

[62] Here we employ the technique developed in the previous section, using the range of markers for primary and secondary processes provided by the VOC data set to define the characteristic OC:EC primary emission ratio for the Pittsburgh region in summer and winter. This approach avoids the need to carefully select time periods that will yield the "correct" value of $(OC/EC)_E$. In addition, the suite of primary and secondary VOCs available provides bounds on the value of $(OC/EC)_E$ appropriate to a given time period. The secondary organic aerosol is then calculated according to (6).

[63] The coefficient of determination between M_o and combustion and photochemically derived VOCs is shown in Figure 8 as a function of $(OC/EC)_E$ for winter and summer. Again, the critical point of the curves gives the representative value of $(OC/EC)_E$ for that time of year.

[64] The median value of $(OC/EC)_E$ determined for the winter data set was 1.85 (IQR: 1.82–1.86), whereas that for the summer data set was lower with a median of 1.36 (IQR: 1.27–1.48) (Table 5). Substantially higher particulate concentrations of levoglucosan were observed in the winter, indicative of increased wood combustion. More widespread wood burning is a likely cause of the higher primary OC:EC emission ratio at that time of year. Colder engines and less efficient combustion may have also contributed to the higher wintertime ratio.

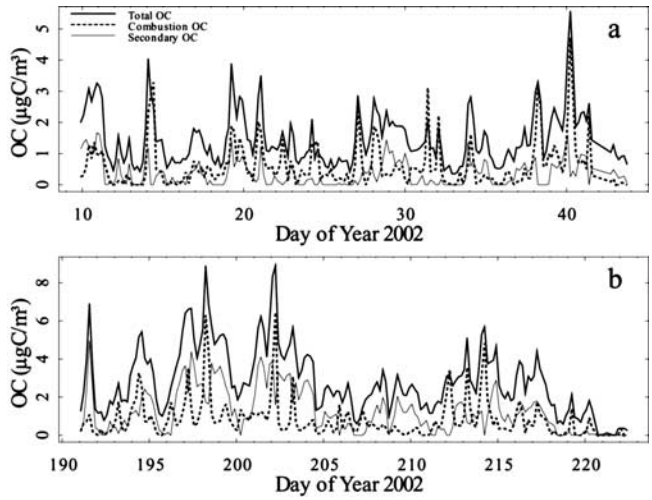

Figure 9. Timelines of total OC (M_{oc}, μgC/m^3), dark solid line; combustion OC (M_c, μgC/m^3), dashed line; secondary OC (M_o, μgC/m^3), light solid line. Data are shown for the (a) winter and (b) summer deployments.

[65] Using the derived values of $(OC/EC)_E$ for summer and winter, we can then calculate M_o, the secondary OC, according to (6). Timelines of the total (M_{oc}), combustion (M_c), and secondary (M_o) aerosol organic carbon concentrations (in μgC/m^3) for winter and summer 2002 are plotted in Figure 9, and quantiles of these quantities are given in Table 5. Note that since M_c is defined as $M_{ec}(OC/EC)_E$, there are occasional episodes where $M_c > M_{oc}$. Negative values of M_o were assumed to contain no secondary material and were set to zero.

[66] Ambient concentrations of aerosol organic carbon in the summer experiment were on average twice as high as in the winter (Table 5). Background levels (M_a) made up a significant fraction of the total ambient aerosol OC concentrations in both seasons. Background aerosol OC concentrations were slightly higher in summer but a larger fraction of the total in winter (median of 49% versus 35%). Similarly, combustion OC was slightly higher in the summer, however, it made up a larger fraction of the total OC in winter (median of 30% versus 19%). Secondary organic carbon (M_o) accounted for a median of 16% (IQR: 0–35%) of the aerosol OC in winter, and 37% (IQR: 15–56%) in summer (Table 5).

[67] A. Polidori et al. (manuscript in preparation, 2005) carried out an analysis of the primary and secondary components of OC in Pittsburgh during the PAQS study

Table 5. OC Combustion Emission Ratios and Source Contributions[a]

	Ambient Concentration		Primary Emission Ratio		Background Concentration			Combustion Emissions				Secondary Production			
	M_{oc}, μgC/m^3		$(OC/EC)_E$		M_a, μgC/m^3	M_a/M_{oc}		M_c, μgC/m^3		M_c/M_{oc}		M_o, μgC/m^3		M_o/M_{oc}	
Season	Median	IQR[b]	Median	IQR[b]		Median	IQR[b]	Median	IQR[b]	Median	IQR[b]	Median	IQR[b]	Median	IQR[b]
Winter	1.2	0.83–2.0	1.85	1.82–1.86	0.60	0.49	0.30–0.72	0.37	0.13–0.75	0.30	0.13–0.48	0.20	0.00–0.59	0.16	0.00–0.35
Summer	2.5	1.6–3.9	1.36	1.27–1.48	0.87	0.35	0.22–0.54	0.50	0.20–1.1	0.19	0.10–0.32	0.99	0.27–1.9	0.37	0.15–0.56

[a]Note that the median values of the source contributions do not necessarily add up to the median ambient concentration as the median is not a distributive property.
[b]IQR, interquartile range.

using the *Turpin and Huntzicker* [1995] EC tracer method. For overlapping time periods (10 January to 12 February and 10–31 July 2002), they calculate median secondary OC concentrations of 0.21 $\mu gC/m^3$ (15% of total OC) and 1.04 $\mu gC/m^3$ (47% of total OC) respectively. These values are in good agreement with those calculated here for the same periods: 0.20 $\mu gC/m^3$ (16% of total OC) and 1.15 $\mu gC/m^3$ (43% of total OC) (note that these values differ slightly from those in Table 5 since they do not reflect identical time periods).

3.4. Characterization of the Chemical State of the Atmosphere: VOC Contributions to OH Loss

[68] Photochemical production of secondary organic aerosol (SOA) depends on the chemical state of the atmosphere, both in terms of oxidative capacity, and in term of the quantity and nature of gas phase organic material that is present to form aerosol. In this section we describe the relative importance of different classes of VOCs to tropospheric photochemistry in the Pittsburgh region in summer and winter, and show that higher levels of photochemically active compounds are present in summer, when SOA levels are highest, due to biogenic emissions and photochemical production of OVOCs.

[69] A useful measure of air mass chemical reactivity is the OH loss rate (L_{OH}, s^{-1}), defined as

$$L_{OH} = \sum_i k_i \chi_i, \quad (7)$$

where k_i is the reaction rate constant for species i with the hydroxyl radical [*Atkinson*, 1994], and χ_i is the concentration of i in molec/cm^3. L_{OH} has units of s^{-1} and represents the inverse lifetime of the hydroxyl radical with respect to reaction with the measured compounds.

[70] Daytime (1000–1600 EST) values of L_{OH} were calculated for the following groups of compounds: total (all measured VOCs plus CO); alkanes; alkenes + alkynes; aromatics; OVOCs; isoprene plus its oxidation products methacrolein, methylvinylketone, and 3-methylfuran; and CO (Figure 10; Tables 6 and 7).

[71] Due to analytical challenges, VOC measurements in many field studies of air quality and atmospheric chemistry comprise only the anthropogenic nonmethane hydrocarbons (NMHCs; alkanes, alkenes, alkynes and aromatics). In Pittsburgh during January and February 2002, these species accounted for a substantial portion (approximately 60%) of the total measured OH loss rate. However, while their collective OH reactivity was only slightly less in summer (0.68 s^{-1} versus 0.89 s^{-1}), their importance relative to other VOCs was dramatically lower, as they accounted for only 11% on average of total L_{OH} during summer. Similarly, the CO reactivity was comparable in both seasons (median of 0.49 s^{-1} in winter and 0.53 s^{-1} in summer), but its relative contribution to the total measured OH loss rate was much greater in winter (median of 23% versus 7% in the summer). It should be pointed out that these calculations do not include the C_2 hydrocarbons ethane, ethene and ethyne, which were not measured. Based on published ratios of these compounds to other species [*Parrish et al.*, 1998], we estimate that they would cause an OH loss rate of approximately 0.05 s^{-1} and 0.13 s^{-1} for summer and winter.

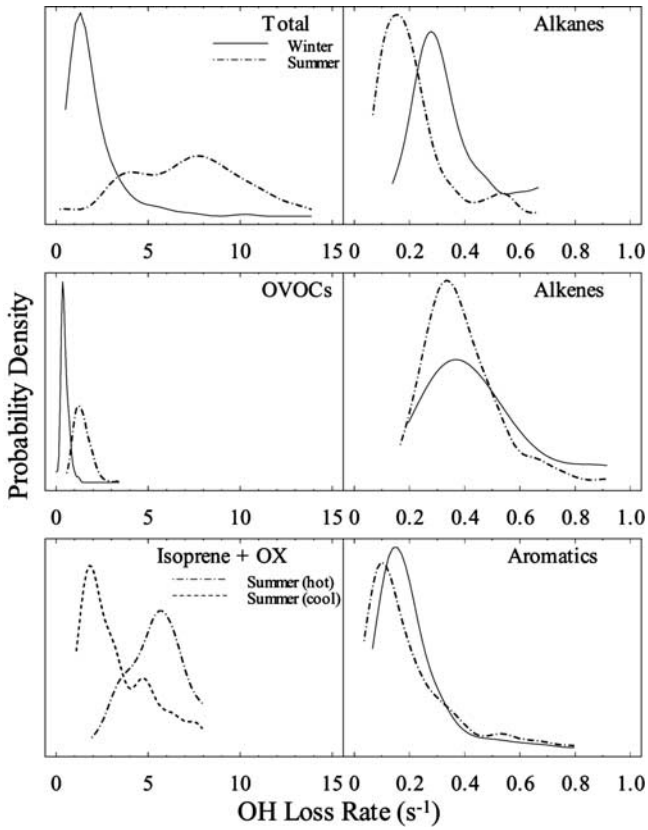

Figure 10. Probability density curves of measured daytime (1000–1600 EST) VOC OH loss rate by compound class for winter and summer 2002. Measured OH loss rate for isoprene plus its oxidation products methacrolein, methylvinylketone, and 3-methylfuran is shown for both hot (maximum air temperature $\geq$ 29°C) and cool (maximum air temperature < 29°C) days in the summer. These compounds were not present above detection limit in the winter. Note the different scales for the x axes in the left- and right-hand columns.

[72] Despite the comparable NMHC and CO reactivity in the two seasons, the total measured daytime OH loss rate underwent a more than fourfold increase from winter (median = 1.42 s^{-1}; IQR: 1.12–2.30 s^{-1}) to summer (median = 7.25 s^{-1}; IQR: 4.60–9.38 s^{-1}). This was due to the presence of high levels of isoprene and its oxidation products in summer, and also to the three-fold increase in oxygenated VOC concentration and reactivity from winter to summer (Tables 6, 7). Isoprene plus its oxidation products accounted for a median of 62% (IQR: 52–70%) of the daytime OH loss rate in summer, with the OVOCs accounting for an additional 20% (IQR: 15–26%). Formaldehyde measurements were not made during the PAQS study, and including the effects of this compound would result in an increased contribution to the calculated OH loss rate from the OVOCs in both seasons.

[73] The PAQS sampling site was located at the north end of Schenley Park, a 456 acre urban park with substantial tree cover. To test whether the observed isoprene concentrations were biased by the presence of a large nearby source, the daytime OH loss due to isoprene and its

Table 6. Quantiles of Daytime OH Loss Rate: Winter Data[a,b]

	All Days				High Ozone Days[c]			
	L_{OH}, s^{-1}		Fraction of Total VOC L_{OH}		L_{OH}, s^{-1}		Fraction of Total VOC L_{OH}	
Category	Median	IQR[e]	Median	IQR[e]	Median	IQR[e]	Median	IQR[e]
Total	1.42	1.12–2.30			1.00	0.91–1.27		
Alkanes[f]	0.31	0.25–0.41	0.20	0.17–0.25	0.27	0.17–0.32	0.20	0.18–0.26
Alkenes + Alkynes[f]	0.41	0.32–0.57	0.27	0.23–0.32	0.29	0.23–0.40	0.25	0.22–0.30
Aromatics	0.17	0.12–0.23	0.11	0.09–0.13	0.12	0.09–0.19	0.10	0.09–0.12
OVOCs	0.41	0.33–0.57	0.29	0.23–0.35	0.45	0.31–0.54	0.38	0.29–0.45
CO	0.49	0.21–1.05	0.23	0.17–0.36	0.19	0.19–0.19	0.20	0.20–0.22
	High OC Days[c]				Nucleation Days[d]			
	L_{OH}, s^{-1}		Fraction of Total VOC L_{OH}		L_{OH}, s^{-1}		Fraction of Total VOC L_{OH}	
Category	Median	IQR[e]	Median	IQR[e]	Median	IQR[e]	Median	IQR[e]
Total	2.70	1.64–3.35			1.04	0.98–1.20		
Alkanes[f]	0.40	0.33–0.58	0.18	0.14–0.20	0.26	0.24–0.30	0.27	0.21–0.29
Alkenes + alkynes[f]	0.57	0.44–0.84	0.24	0.20–0.30	0.28	0.26–0.35	0.28	0.25–0.31
Aromatics	0.25	0.14–0.31	0.09	0.07–0.11	0.12	0.10–0.16	0.11	0.09–0.13
OVOCs	0.69	0.51–0.78	0.26	0.21–0.32	0.37	0.34–0.45	0.35	0.32–0.38
CO	0.74	0.45–1.56	0.28	0.16–0.36	<DL[g]	<DL[g]	<DL[g]	<DL[g]

[a]Note that the median values of the components do not necessarily add up to the median of the total as the median is not a distributive property.
[b]Daytime: 1000–1600 EST.
[c]High ozone and high OC days are defined as days when the daily maximum concentration was above the 0.8 quantile for all daily maxima.
[d]Days on which moderate to strong nucleation events occurred [*Stanier et al.*, 2004b].
[e]IQR, interquartile range.
[f]Note that ethane, ethene, and ethyne were not measured. See text for discussion.
[g]CO concentrations during these periods were below the instrumental detection limit of 0.1 ppm.

oxidation products was calculated for time periods when the wind was only from the northern sector and the wind speed was greater than 1 m/s. The resulting OH loss rate (median 4.55 s^{-1}; IQR 2.85–5.73 s^{-1}) was not significantly different from that calculated using all of the daytime data (median 4.71 s^{-1}; IQR 2.77–6.20 s^{-1}). Hence we find that in winter, the total daytime OH loss rate is dominated by the nonmethane hydrocarbons and CO, whereas in summer it is dominated by isoprene, its oxidation products, and oxygenated VOCs. The above calculations do not include methane,

Table 7. Quantiles of Daytime OH Loss Rate: Summer Data[a,b]

	All Days				High Ozone Days[c]			
	L_{OH}, s^{-1}		Fraction of Total VOC L_{OH}		L_{OH}, s^{-1}		Fraction of Total VOC L_{OH}	
Category	Median	IQR[e]	Median	IQR[e]	Median	IQR[e]	Median	IQR[e]
Total	7.25	4.60–9.38			8.53	7.17–9.77		
Alkanes[f]	0.17	0.12–0.24	0.03	0.02–0.04	0.19	0.17–0.30	0.03	0.02–0.04
Alkenes + alkynes[f]	0.36	0.30–0.45	0.06	0.04–0.07	0.42	0.36–0.51	0.05	0.04–0.06
Aromatics	0.14	0.08–0.24	0.02	0.01–0.04	0.13	0.08–0.24	0.02	0.01–0.03
OVOCs	1.35	1.09–1.64	0.20	0.15–0.26	1.80	1.53–1.97	0.21	0.16–0.24
Isop + Ox[f]	4.71	2.77–6.20	0.62	0.52–0.70	5.69	3.75–6.67	0.63	0.58–0.71
CO	0.53	0.26–0.86	0.07	0.04–0.12	0.60	0.24–0.83	0.06	0.03–0.09
	High OC Days[c]				Nucleation Days[d]			
	L_{OH}, s^{-1}		Fraction of Total VOC L_{OH}		L_{OH}, s^{-1}		Fraction of Total VOC L_{OH}	
Category	Median	IQR[e]	Median	IQR[e]	Median	IQR[e]	Median	IQR[e]
Total	9.26	8.23–10.43			4.96	3.37–6.47		
Alkanes[f]	0.21	0.16–0.27	0.03	0.02–0.04	0.11	0.09–0.20	0.03	0.02–0.03
Alkenes + alkynes[f]	0.38	0.31–0.48	0.04	0.04–0.06	0.35	0.25–0.43	0.07	0.06–0.07
Aromatics	0.27	0.19–0.40	0.03	0.02–0.05	0.12	0.08–0.14	0.02	0.02–0.03
OVOCs	1.54	1.35–1.84	0.17	0.14–0.20	1.30	1.05–1.59	0.26	0.23–0.30
Isop + Ox[g]	5.71	4.58–6.75	0.64	0.57–0.70	3.16	1.91–3.92	0.59	0.52–0.62
CO	0.71	0.57–1.04	0.09	0.07–0.11	0.22	0.16–0.54	0.07	0.02–0.09

[a]Note that the median values of the components do not necessarily add up to the median of the total as the median is not a distributive property.
[b]Daytime: 1000–1600 EST.
[c]High ozone and high OC days are defined as days when the daily maximum concentration was above the 0.8 quantile for all daily maxima.
[d]Days on which moderate to strong nucleation events occurred [*Stanier et al.*, 2004b].
[e]IQR, interquartile range.
[f]Note that ethane, ethene, and ethyne were not measured. See text for discussion.
[g]Isoprene plus its oxidation products MACR, MVK, and 3-methylfuran.

which was not measured during the experiment. Based on background concentrations of methane at this latitude (see http://www.cmdl.noaa.gov/info/ftpdata.html), we estimate the OH loss rate in Pittsburgh due to methane at approximately 0.21 s^{-1} during the winter and 0.32 s^{-1} during the summer.

[74] Daytime OH loss rates were also calculated on the following subsets of the data: high ozone days, high aerosol OC days, and days in which moderate to strong nucleation events were observed [*Stanier et al.*, 2004b] (Tables 6 and 7). High ozone and high OC days were defined as days in which the maximum value of these quantities was above the 0.8 quantile for all observed daily maxima.

[75] For July and August, the 0.8 concentration quantile for the daily maximum ozone was 84 ppb. On high ozone days, the total measured OH loss rate was higher (median: 8.53 s^{-1}) than otherwise (days not exceeding this threshold had a median OH loss rate of 6.74 s^{-1}), and this increase was distributed relatively evenly among the different compound classes (Table 7). During January and February, the 0.8 quantile for daily ozone maxima was only 30 ppb. Days during which ozone exceeded this amount had a lower overall OH loss rate (median 1.00 s^{-1}) than days on which it did not (median 1.57 s^{-1}). These higher ozone days in the winter may have occurred during periods of enhanced vertical mixing. *Comrie and Yarnal* [1992] analyzed the dependence of surface ozone in Pittsburgh on synoptic climatology. They concluded that high ozone levels in summer developed under stagnant anticyclonic conditions, whereas in winter high ozone concentrations were associated with tropopause folding and vertical transport of stratospheric ozone.

[76] In both seasons, days with high OC loadings were associated with higher levels of all VOC compound categories and CO. In January–February, the median OH loss rate was 2.70 s^{-1} on days with high OC versus 1.28 s^{-1} on days without. In July–August, the median daytime OH loss rate was 9.26 s^{-1} on high OC days and 6.81 s^{-1} on other days. By contrast, days on which nucleation events occurred had lower overall OH loss rates (medians of 1.04 s^{-1} and 4.96 s^{-1} in winter and summer, respectively) than days without nucleation events (medians of 1.54 s^{-1} and 7.93 s^{-1} in winter and summer). *Stanier et al.* [2004b] found that the occurrence of nucleation events during PAQS was dependent on the preexisting aerosol surface area available for condensation. The lower OH loss rates on nucleation days may be due to a positive correlation between gas phase reactivity and aerosol surface area (r^2 = 0.48 in winter and 0.28 in summer); i.e. less polluted days with low OH loss rates also had lower particle surface area available for condensation of semivolatile aerosol precursors, which increased the likelihood of new particle nucleation.

4. Conclusions

[77] High temporal density speciated VOC measurements provide a useful framework for interpreting aerosol measurements. Statistical analyses such as factor analysis on combined VOC-aerosol data sets can test precepts used in source-receptor modeling. The range of combustion and photochemical markers in the VOC data set also enables us to deconvolve the relative contributions to ambient levels of OVOCs and aerosol OC from different source types. We calculate that secondary plus biogenic sources accounted for 24%, 12% and 27% of the ambient concentrations of acetone, MEK and acetaldehyde respectively in the winter and 29%, 26% and 34% respectively in the summer. Aerosol OC was found to be composed of 16% secondary carbon in the winter and 37% secondary carbon in the summer. The importance of the background contribution to observed concentrations of both OVOCs and aerosol OC emphasizes the role of longer-range transport and the need for a regional perspective in addressing air quality concerns. While local automotive emissions were the primary factor driving changes in VOC concentrations in Pittsburgh, they did not contribute significantly to variability in the aerosol species included in the factor analysis (PM 2.5 mass, aerosol sulfate and nitrate mass, and aerosol number density).

[78] VOC concentration data can also help define chemical conditions that are conducive to particle formation and growth. We find that while aerosol OC loadings are highest when VOC concentrations and reactivities are high, nucleation events tended to occur on days when levels of VOCs and CO were low. High ozone days in the summer were associated with high OH loss rates due to the VOCs and CO, whereas in the winter the highest ozone levels occurred on days with low levels of CO and nonmethane hydrocarbons but slightly higher OVOC concentrations.

[79] One of the overall objectives of the PAQS study is to develop the ability to predict changes in PM characteristics and atmospheric composition due to proposed changes in emissions. Reaching this objective will require accurate modeling of the chemical and dynamical processes controlling atmospheric composition in the Pittsburgh region. The results presented here should help to provide a basis upon which to test mechanisms included in such models.

[80] **Acknowledgments.** This research was conducted as part of the Pittsburgh Air Quality Study, which was supported by the US EPA under contract R82806101 and the US DOE National Energy Technology Laboratory under contract DE-FC26-01NT41017. DBM thanks the DOE for a GREF fellowship. The authors thank all of the PAQS researchers for their help; in particular, Allen Robinson, Beth Wittig, and Andrey Khlystov. Thanks also to Megan McKay for her considerable help.

References

Atkinson, R. (1994), Gas phase tropospheric chemistry of organic compounds, *J. Phys. Chem. Ref. Data Monogr.*, *2*, 1–216.

Bakwin, P. S., D. F. Hurst, P. P. Tans, and J. W. Elkins (1997), Anthropogenic sources of halocarbons, sulfur hexafluoride, carbon monoxide, and methane in the southeastern United States, *J. Geophys. Res.*, *102*(D13), 15,915–15,925.

Barnes, D. H., S. C. Wofsy, B. P. Fehlau, E. W. Gottlieb, J. W. Elkins, G. S. Dutton, and S. A. Montzka (2003), Urban/industrial pollution for the New York City–Washington, D. C., corridor, 1996–1998: 1. Providing independent verification of CO and PCE emissions inventories, *J. Geophys. Res.*, *108*(D6), 4185, doi:10.1029/2001JD001116.

Cabada, J. C., S. N. Pandis, and A. L. Robinson (2002), Sources of atmospheric carbonaceous particulate matter in Pittsburgh, Pennsylvania, *J. Air Waste Manage.*, *52*(6), 732–741.

Cabada, J. C., S. Takahama, A. Khlystov, S. N. Pandis, S. Rees, C. I. Davidson, and A. L. Robinson (2004), Mass size distributions and size resolved chemical composition of fine particulate matter at the Pittsburgh Supersite, *Atmos. Environ.*, *38*(20), 3127–3141.

Comrie, A. C., and B. Yarnal (1992), Relationships between synoptic-scale atmospheric circulation and ozone concentrations in metropolitan Pittsburgh, Pennsylvania, *Atmos. Environ.*, *26*(3), 301–312.

Czoschke, N. M., M. Jang, and R. M. Kamens (2003), Effect of acidic seed on biogenic secondary organic aerosol growth, *Atmos. Environ.*, *37*(30), 4287–4299.

Fraser, M. P., G. R. Cass, and B. R. T. Simoneit (1998), Gas-phase and particle-phase organic compounds emitted from motor vehicle traffic in a Los Angeles roadway tunnel, *Environ. Sci. Technol.*, *32*(14), 2051–2060.

Goldan, P. D., M. Trainer, W. C. Kuster, D. D. Parrish, J. Carpenter, J. M. Roberts, J. E. Yee, and F. C. Fehsenfeld (1995a), Measurements of hydrocarbons, oxygenated hydrocarbons, carbon monoxide, and nitrogen oxides in an urban basin in Colorado: Implications for emission inventories, *J. Geophys. Res.*, *100*(D11), 22,771–22,783.

Goldan, P. D., W. C. Kuster, F. C. Fehsenfeld, and S. A. Montzka (1995b), Hydrocarbon measurements in the southeastern United States: The Rural Oxidants in the Southern Environment (ROSE) program 1990, *J. Geophys. Res.*, *100*(D12), 25,945–25,963.

Goldstein, A. H., and G. W. Schade (2000), Quantifying biogenic and anthropogenic contributions to acetone mixing ratios in a rural environment, *Atmos. Environ.*, *34*(29–30), 4997–5006.

Goldstein, A. H., B. C. Daube, J. W. Munger, and S. C. Wofsy (1995a), Automated in-situ monitoring of atmospheric non-methane hydrocarbon concentrations and gradients, *J. Atmos. Chem.*, *21*(1), 43–59.

Goldstein, A. H., S. C. Wofsy, and C. M. Spivakovsky (1995b), Seasonal variations of nonmethane hydrocarbons in rural New England: Constraints on OH concentrations in northern midlatitudes, *J. Geophys. Res.*, *100*(D10), 21,023–21,033.

Goldstein, A. H., S. M. Fan, M. L. Goulden, J. W. Munger, and S. C. Wofsy (1996), Emissions of ethene, propene, and 1-butene by a midlatitude forest, *J. Geophys. Res.*, *101*(D4), 9149–9157.

Greenberg, J. P., B. Lee, D. Helmig, and P. R. Zimmerman (1994), Fully automated gas chromatograph-flame ionization detector system for the in situ determination of atmospheric nonmethane hydrocarbons at low parts per trillion concentration, *J. Chromatogr. A*, *676*(2), 389–398.

Grosjean, D. (1982), Formaldehyde and other carbonyls in Los Angeles ambient air, *Environ. Sci. Technol.*, *16*(5), 254–262.

Hoffmann, T., R. Bandur, U. Marggraf, and M. Linscheid (1998), Molecular composition of organic aerosols formed in the alpha-pinene/O_3 reaction: Implications for new particle formation processes, *J. Geophys. Res.*, *103*(D19), 25,569–25,578.

Jang, M. S., N. M. Czoschke, S. Lee, and R. M. Kamens (2002), Heterogeneous atmospheric aerosol production by acid-catalyzed particle-phase reactions, *Science*, *298*(5594), 814–817.

Kirchstetter, T. W., B. C. Singer, R. A. Harley, G. B. Kendall, and W. Chan (1996), Impact of oxygenated gasoline use on California light-duty vehicle emissions, *Environ. Sci. Technol.*, *30*(2), 661–670.

Kirchstetter, T. W., B. C. Singer, R. A. Harley, G. R. Kendall, and J. M. Hesson (1999), Impact of California reformulated gasoline on motor vehicle emissions. 2. Volatile organic compound speciation and reactivity, *Environ. Sci. Technol.*, *33*(2), 329–336.

Koch, S., R. Winterhalter, E. Uherek, A. Kolloff, P. Neeb, and G. K. Moortgat (2000), Formation of new particles in the gas-phase ozonolysis of monoterpenes, *Atmos. Environ.*, *34*(23), 4031–4042.

Lamanna, M. S., and A. H. Goldstein (1999), In situ measurements of C_2–C_{10} volatile organic compounds above a Sierra Nevada ponderosa pine plantation, *J. Geophys. Res.*, *104*(D17), 21,247–21,262.

Lim, H. J., and B. J. Turpin (2002), Origins of primary and secondary organic aerosol in Atlanta: Results of time-resolved measurements during the Atlanta Supersite experiment, *Environ. Sci. Technol.*, *36*(21), 4489–4496.

McKeen, S. A., and S. C. Liu (1993), Hydrocarbon ratios and photochemical history of air masses, *Geophys. Res. Lett.*, *20*(21), 2363–2366.

Odum, J. R., T. Hoffmann, F. Bowman, D. Collins, R. C. Flagan, and J. H. Seinfeld (1996), Gas/particle partitioning and secondary organic aerosol yields, *Environ. Sci. Technol.*, *30*(8), 2580–2585.

Parrish, D. D., C. J. Hahn, E. J. Williams, R. B. Norton, F. C. Fehsenfeld, H. B. Singh, J. D. Shetter, B. W. Gandrud, and B. A. Ridley (1992), Indications of photochemical histories of Pacific air masses from measurements of atmospheric trace species at Point Arena, California, *J. Geophys. Res.*, *97*(D14), 15,883–15,901.

Parrish, D. D., et al. (1998), Internal consistency tests for evaluation of measurements of anthropogenic hydrocarbons in the troposphere, *J. Geophys. Res.*, *103*(D17), 22,339–22,359.

Riemer, D., et al. (1998), Observations of nonmethane hydrocarbons and oxygenated volatile organic compounds at a rural site in the southeastern United States, *J. Geophys. Res.*, *103*(D21), 28,111–28,128.

Schade, G. W., and A. H. Goldstein (2001), Fluxes of oxygenated volatile organic compounds from a ponderosa pine plantation, *J. Geophys. Res.*, *106*(D3), 3111–3123.

Singh, H. B., M. Kanakidou, P. J. Crutzen, and D. J. Jacob (1995), High concentrations and photochemical fate of oxygenated hydrocarbons in the global troposphere, *Nature*, *378*(6552), 50–54.

Singh, H., Y. Chen, A. Staudt, D. Jacob, D. Blake, B. Heikes, and J. Snow (2001), Evidence from the Pacific troposphere for large global sources of oxygenated organic compounds, *Nature*, *410*(6832), 1078–1081.

Staehelin, J., C. Keller, W. Stahel, K. Schlapfer, and S. Wunderli (1998), Emission factors from road traffic from a tunnel study (Gubrist tunnel, Switzerland). part III: Results of organic compounds, SO_2 and speciation of organic exhaust emission, *Atmos. Environ.*, *32*(6), 999–1009.

Stanier, C. O., A. Y. Khlystov, and S. N. Pandis (2004a), Ambient aerosol size distributions and number concentrations measured during the Pittsburgh Air Quality Study (PAQS), *Atmos. Environ.*, *38*(20), 3275–3284.

Stanier, C. O., A. Y. Khlystov, and S. N. Pandis (2004b), Nucleation events during the Pittsburgh Air Quality Study: Description and relation to key meteorological, gas phase, and aerosol parameters, *Aerosol Sci. Technol.*, *38*(21), 253–264.

Sweet, C. W., and S. J. Vermette (1992), Toxic volatile organic compounds in urban air in Illinois, *Environ. Sci. Technol.*, *26*(1), 165–173.

Thunis, P., and C. Cuvelier (2000), Impact of biogenic emissions on ozone formation in the Mediterranean area—A BEMA modelling study, *Atmos. Environ.*, *34*(3), 467–481.

Tolocka, M. P., P. A. Solomon, W. Mitchell, G. A. Norris, D. B. Gemmill, R. W. Wiener, R. W. Vanderpool, J. B. Homolya, and J. Rice (2001), East versus west in the US: Chemical characteristics of PM2.5 during the winter of 1999, *Aerosol Sci. Technol.*, *34*(1), 88–96.

Turpin, B. J., and J. J. Huntzicker (1995), Identification of secondary organic aerosol episodes and quantitation of primary and secondary organic aerosol concentrations during SCAQS, *Atmos. Environ.*, *29*(23), 3527–3544.

Wittig, B., N. Anderson, A. Y. Khlystov, S. N. Pandis, C. Davidson, and A. L. Robinson (2004a), Pittsburgh Air Quality Study overview and initial scientific findings, *Atmos. Environ.*, *38*(20), 3107–3125.

Wittig, B., S. Takahama, A. Khlystov, S. N. Pandis, S. Hering, B. Kirby, and C. Davidson (2004b), Semicontinuous PM2.5 inorganic composition measurements during the Pittsburgh Air Quality Study, *Atmos. Environ.*, *38*(20), 3201–3213.

Zielinska, B., J. C. Sagebiel, G. Harshfield, A. W. Gertler, and W. R. Pierson (1996), Volatile organic compounds up to C_{20} emitted from motor vehicles: Measurement methods, *Atmos. Environ.*, *30*(12), 2269–2286.

A. H. Goldstein, Department of ESPM-Ecosystem Sciences, University of California, Berkeley, 151 Hilgard Hall, Berkeley, CA 94720, USA. (ahg@nature.berkeley.edu)

N. M. Donahue and S. N. Pandis, Department of Chemical Engineering, Carnegie Mellon University, 5000 Forbes Ave, Pittsburgh, PA 15213, USA.

D. B. Millet, Department of Earth and Planetary Sciences, Harvard University, Pierce Hall, 29 Oxford St., Cambridge, MA 02138, USA. (dbm@io.harvard.edu)

A. Polidori and B. J. Turpin, Department of Environmental Sciences, Rutgers University, 14 College Farm Rd., New Brunswick, NJ 08901, USA.

C. O. Stanier, Department of Chemical and Biochemical Engineering, University of Iowa, 4122 Seamens Center, Iowa City, IA 52242, USA.